ORIGINAL RESEARCH

# Molecular Imaging of Folate Receptor β–Positive Macrophages during Acute Lung Inflammation

Wei Han[1], Rinat Zaynagetdinov[1], Fiona E. Yull[2], Vasiliy V. Polosukhin[1], Linda A. Gleaves[1], Harikrishna Tanjore[1], Lisa R. Young[1,3], Todd E. Peterson[4,5], H. Charles Manning[4,5], Lawrence S. Prince[6], and Timothy S. Blackwell[1,2,7,8]

[1]Division of Allergy, Pulmonary and Critical Care Medicine, Department of Medicine, [2]Department of Cancer Biology, [3]Division of Pulmonary Medicine, Department of Pediatrics, [4]Department of Radiology and Radiological Sciences, [5]Institute of Imaging Science, and [7]Department of Cell and Developmental Biology, Vanderbilt University School of Medicine, Nashville, Tennessee; [6]Division of Neonatology, Department of Pediatrics, University of California, San Diego, La Jolla, California; and [8]Department of Veterans Affairs Medical Center, Nashville, Tennessee

## Abstract

Characterization of markers that identify activated macrophages could advance understanding of inflammatory lung diseases and facilitate development of novel methodologies for monitoring disease activity. We investigated whether folate receptor β (FRβ) expression could be used to identify and quantify activated macrophages in the lungs during acute inflammation induced by *Escherichia coli* LPS. We found that FRβ expression was markedly increased in lung macrophages at 48 hours after intratracheal LPS. *In vivo* molecular imaging with a fluorescent probe (cyanine 5 polyethylene glycol folate) showed that the fluorescence signal over the chest peaked at 48 hours after intratracheal LPS and was markedly attenuated after depletion of macrophages. Using flow cytometry, we identified the cells responsible for uptake of cyanine 5–conjugated folate as FRβ$^+$ interstitial macrophages and pulmonary monocytes, which coexpressed markers associated with an M1 proinflammatory macrophage phenotype. These findings were confirmed using a second model of acute lung inflammation generated by inducible transgenic expression of an NF-κB activator in airway epithelium. Using CC chemokine receptor 2–deficient mice, we found that FRβ$^+$ macrophage/monocyte recruitment was dependent on the monocyte chemotactic protein-1/CC chemokine receptor 2 pathway. Together, our results demonstrate that folate-based molecular imaging can be used as a noninvasive approach to detect classically activated monocytes/macrophages recruited to the lungs during acute inflammation.

**Keywords:** macrophage; folate receptor β; molecular imaging; acute lung inflammation

### Clinical Relevance

This work identifies a new approach for quantifying and monitoring acute lung inflammation based on folate receptor β expression in activated pulmonary monocytes/macrophages. That could be applied for monitoring and investigating pathologies of inflammatory lung diseases in humans.

Macrophages provide the first line of host defense against invaders in the lungs by patrolling the airspaces, phagocytosing particulates and microbes, and activating the inflammatory cascade when necessary. In addition to playing key roles in host defense and initiating the innate immune response, macrophages also participate in resolving inflammation, repairing the lung after injury, and interfacing with cells of the adaptive immune response (1, 2). In response to bacterial products, including LPS, macrophages trigger a cascade of events mediated through the NF-κB pathway, resulting in production of proinflammatory cytokines or chemokines, including TNF-α and IL-1β (2, 3). Persistent macrophage activation prevents

(Received in original form July 23, 2014; accepted in final form October 31, 2014)

This work was supported by National Institutes of Health grants HL094296, HL119503, HL 085317, and HL116358, and by the U.S. Department of Veterans Affairs.

Author Contributions: study conception and design—W.H., L.S.P., and T.S.B.; data acquisition—W.H., R.Z., V.V.P., L.A.G., and H.T.; drafting or revising the manuscript—W.H., F.E.Y., L.R.Y., T.E.P., H.C.M., L.S.P., and T.S.B.

Correspondence and requests for reprints should be addressed to Wei Han, M.D., Division of Allergy, Pulmonary, and Critical Care Medicine, Vanderbilt University Medical Center, T-1217 MCN, 1161 21st Avenue, Nashville, TN 37232. E-mail: wei.han@vanderbilt.edu

This article has an online supplement, which is accessible from this issue's table of contents at www.atsjournals.org

Am J Respir Cell Mol Biol Vol 53, Iss 1, pp 50–59, Jul 2015

Originally Published in Press as DOI: 10.1165/rcmb.2014-0289OC on November 6, 2014
Internet address: www.atsjournals.org

resolution of lung inflammation, leading to progressive lung injury (4) and development of acute respiratory distress syndrome in humans (5–7). Development of molecular strategies for detection of sustained macrophage activation could prove valuable for: (*1*) monitoring progression of inflammatory lung diseases, including acute lung injury and acute respiratory distress syndrome; (*2*) better characterizing mechanistic roles of macrophages in inflammatory lung diseases; and (*3*) delineating groups of patients who could benefit from novel antiinflammatory– or macrophage-targeted therapies.

Exposure to microbial stimuli and tissue injury has been reported to increase the expression of unique receptors on the surface of activated macrophages, including receptors for folic acid uptake (8–12). Folic acid is an essential nutrient that functions within the cell to carry one-carbon groups for methylation reactions and for nucleic acid synthesis (13). Several mechanisms have evolved for uptake of folate in eukaryotic cells. A low-affinity, high-capacity transporter, called the reduced folate carrier, is ubiquitously expressed in mammalian cells, and a proton-coupled folate transporter is expressed in kidney and gastrointestinal tract that functions primarily at low pH (14). In addition, there are specific glycophosphoinositol anchored cell surface receptors that bind folate with high affinity, including folate receptor (FR) α and FRβ (14). Whereas FRα is restricted to epithelial cells of the kidney, retina, and choroid plexus, FRβ is expressed in placenta, spleen, and thymus (15). Expression of FRβ has also been detected in leukocytes, including a subset of activated macrophages. Macrophage-specific FRβ expression has been documented in several inflammatory models and diseases, including rheumatoid arthritis, osteoarthritis, lupus, and cancer (11, 15, 16). Although FRβ has not been studied in the context of acute lung inflammation, expression of this functional, high-affinity FR has proven useful for imaging and targeted therapeutic agent development in other disease settings (10, 12, 16, 17, 18).

In the current study, we evaluated expression of FRβ by lung leukocytes during airway inflammation induced by gram-negative bacterial LPS or using transgenic mice with inducible NF-κB activation in airway epithelium. During lung inflammation, we found that FRβ

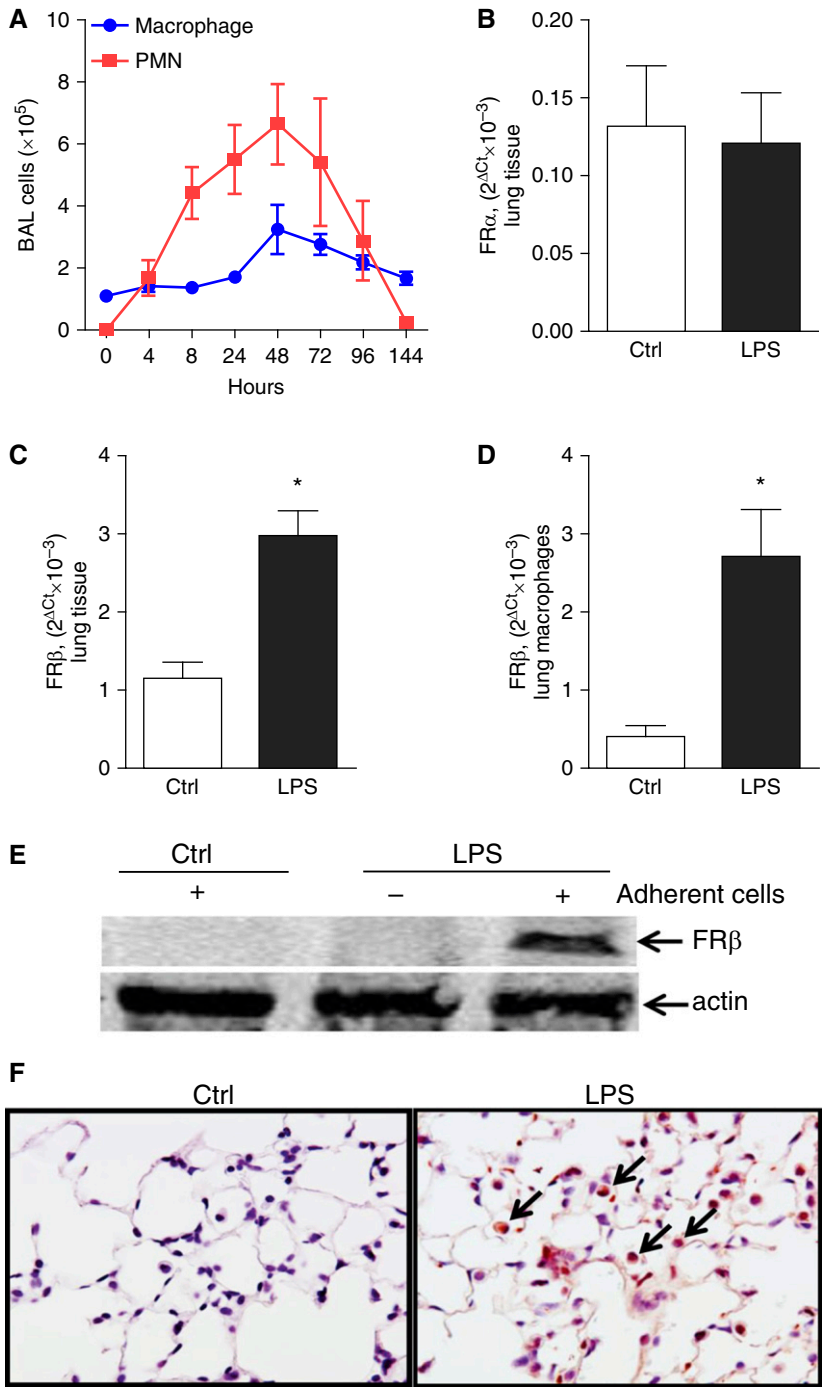


**Figure 1.** Lung macrophages express increased folate receptor (FR) β after LPS stimulation. (*A*) Time course for macrophages and neutrophils in bronchoalveolar lavage (BAL) after intratracheal injection of LPS (3 μg/g body weight; $n = 4$–11 mice per time point). (*B* and *C*) Relative messenger RNA (mRNA) expression of FRα and FRβ in the lungs from mice at 48 hours after intratracheal PBS (Ctrl) or intratracheal LPS (3 μg/g body weight). (*D*) Relative mRNA expression of FRβ and (*E*) Western blot analysis for FRβ in whole-cell lysate or lung macrophages isolated from mice at 48 hours after intratracheal PBS (Ctrl) or intratracheal LPS (3 μg/g body weight). The relative mRNA expression was presented as $2^{\Delta}$ (Ct [housekeeping gene] − Ct [target gene]), where Ct is cycle threshold. Each point represents the mean ± SEM; $n = 3$–4 per group; $^*P < 0.05$. (*F*) Immunostaining for FRβ expression in lung sections (FRβ positive macrophages [*arrows*]) from Ctrl and LPS-treated mice (48 h). PMN, polymorphonuclear leukocytes.

expression is up-regulated specifically in interstitial macrophages and inflammatory lung monocytes with M1 proinflammatory characteristics. We then employed a fluorophore-conjugated folate derivative to demonstrate that folate uptake via FRβ is a robust target for quantitative molecular imaging of monocyte/macrophage activation during acute lung inflammation.

## Materials and Methods

### Animal Models

FVB, C57BL/6 mice, and CC chemokine receptor (CCR) 2 knockout (KO) mice (C57BL/6 background) were purchased from the Jackson Laboratory (Bar Harbor, ME). IKKβ *trans*-activated (IKTA) mice expressing constitutively active IKKβ in Clara cell–specific protein–expressing airway epithelium after doxycycline (dox) treatment have been reported previously (19). Mice were anesthetized with isoflurane and *Escherichia coli* LPS (serotype 055:B5; Sigma-Aldrich, St. Louis, MO) diluted in sterile PBS was administered intratracheally (3 μg/g body weight) after intubation, as previously described (20, 21). All animal care and experimental procedures were conducted according to guidelines issued by the Institutional Animal Care and Use Committee of Vanderbilt University (Nashville, TN).

### Isolation of Lung Macrophages

Lungs were perfused with PBS and digested in RPMI-1640 media containing collagenase XI (0.7 mg/ml; Sigma-Aldrich) and type IV bovine pancreatic DNase (30 μg/ml; Sigma-Aldrich) to obtain single-cell suspensions. After treatment with RBC Lysis Buffer (BioLegend, San Diego, CA), single-cell suspensions were cultured for 2 hours in 100-mm cell culture dishes in RPMI-1640 media supplemented with 10% FBS for collection of adherent macrophages.

### Real-Time Quantitative PCR

RNA was isolated using RNeasy Mini Kit (Qiagen, Valencia, CA), digested with DNase (Ambion, Austin, TX) and reverse transcribed into cDNA by iScript cDNA Synthesis Kit (Bio-Rad, Hercules, CA). Real-time PCR was performed using iQ SYBR Green Supermix (Bio-Rad). Relative messenger RNA (mRNA) expression in each sample was normalized to glyceraldehyde 3-phosphate dehydrogenase and presented using the comparative ΔΔ cycle threshold method.

### Fluorescence Imaging

Cyanine 5 polyethylene glycol folate (Cy5-PEG-folate) and Cy5-PEG–N-hydroxysuccinimide (NHS; where NHS is the control probe) were purchased from Nanocs Inc. (New York, NY) (excitation wavelength, 650 nm; emission, 670 nm). Probes were injected intratracheally or intravenously by retro-orbital injection (500 nmol/kg), and fluorescent imaging was performed with an IVIS 200 system device (Xenogen Corp., Alameda, CA) or a Pearl Impulse system (LI-COR, Lincoln, NE). Data were collected and analyzed using Living Image software version 4.1 (Xenogen) or Pearl Impulse software (LI-COR). Some mice were killed after *in vivo* imaging, and lungs were removed and placed on a black plate for *ex vivo* imaging.

### Depletion of Macrophages with Liposomal Clodronate

Clodronate (dichloromethylene diphosphonic acid; Sigma-Aldrich) or sterile

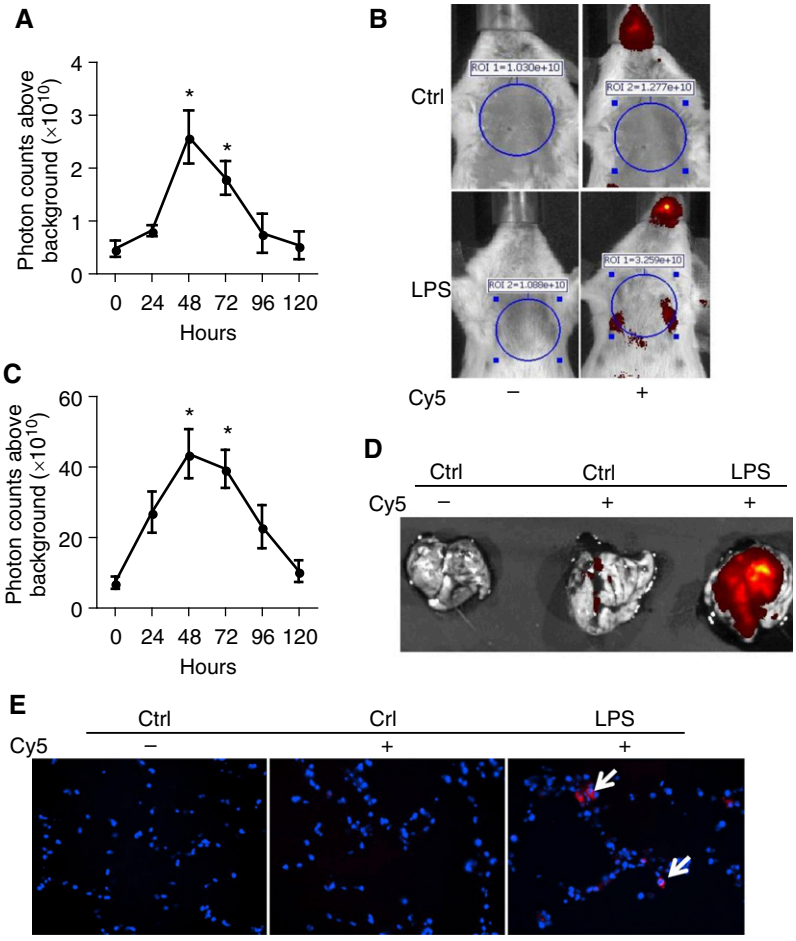


**Figure 2.** LPS treatment increases folate polyethylene glycol cyanine 5 (folate-PEG-Cy5)–derived lung fluorescence in mice. (*A*) Time course of folate-PEG-Cy5–derived chest fluorescence in mice treated with intratracheal LPS (3 μg/g body weight). Images were taken at 1 hour after intratracheal injection of folate-PEG-Cy5 (500 nmol/kg), and photon counts were normalized to background fluorescence (mice were imaged before the injection of intratracheal folate-PEG-Cy5). (*B*) Representative imaging showing chest background fluorescence (no folate probe) and fluorescence at 1 hour after intratracheal injection of folate-PEG-Cy5 (500 nmol/kg; *red*) in ctrl and at 48 hours after intratracheal LPS. Fluorescent signal is detected in the region of the head owing to the method of intratracheal fluorescent probe delivery. (*C*) Time course of folate-PEG-Cy5–derived *ex vivo* lung fluorescence after intratracheal LPS (each point represents the mean ± SEM; $n = 3$–7 per time point; $^*P < 0.05$ compared with baseline [0 h]). (*D*) Representative images demonstrating folate-PEG-Cy5–derived lung fluorescence at 48 hours after intratracheal LPS or PBS (Ctrl). (*E*) Representative images obtained by fluorescence confocal microscopy from frozen sections of control and LPS-treated lungs showing uptake of folate-PEG-Cy5 (*red*) by lung cells with the appearance of macrophages (*arrows*) at 48 hours after LPS treatment. Nuclei are counterstained with 4′,6-diamidino-2-phenylindole.

PBS–containing liposomes were prepared as previously described (22). Mice were treated with clodronate (or PBS control) by intratracheal (75 μl) and intravenous (100 μl) injection 48 hours before injection of LPS.

### Flow Cytometry and Sorting of FRβ$^+$ and FRβ$^-$ Leukocytes

Single-cell suspensions from lung tissue were incubated with Fc receptor block (1 μg/1 × $10^6$ cells; BD Bioscience, San Diego, CA) to reduce nonspecific antibody binding. Dead cells were excluded using Live/Dead Fixable Blue Dead Cell Stain kit (Life Technologies, Carlsbad, CA). Flow cytometry was performed using BD LSR II flow cytometer (BD Bioscience), and data were analyzed with FlowJo software (TreeStar, Ashland, OR).

### Statistical Analysis

Statistical analyses were performed with GraphPad Prism software version 5.04 for Windows (GraphPad Software, La Jolla, CA) using unpaired *t* test for comparisons between two groups ($\alpha = 0.05$) and two-way ANOVA with Bonferroni's post test for comparisons between groups of mice at multiple time points.

## Results

### Intratracheal LPS Results in Increased FRβ Expression in Lung Macrophages

To evaluate expression of FRβ in the lungs, we used the well-characterized model of airway inflammation induced by intratracheal injection of LPS, which results in early recruitment of neutrophils to the lungs followed by a monocyte/macrophage influx that resolves by 7 days (23). Initially, we performed a time course study to evaluate the influx of inflammatory cells into the lungs in this model, and detected an increase in macrophages and neutrophils in bronchoalveolar lavage with maximal values at 48 hours after LPS, followed by reduction at later time points (Figure 1A). Based on these results, we examined FR expression in the lungs at 48 hours after intratracheal LPS. Although intratracheal LPS treatment did not alter expression of FRα in mouse lungs (Figure 1B), we detected increased mRNA expression of FRβ in lung tissue and isolated lung macrophages (Figures 1C and 1D). FRβ expression in lung macrophages was markedly increased at 48 hours after intratracheal LPS, as determined by Western blot (Figure 1E). Consistent with these findings, immunostaining for FRβ revealed very few FRβ-positive cells in lung parenchyma of untreated control mice; however, many FRβ-positive cells were present in lungs at 48 hours after intratracheal LPS (Figure 1F). Together, our results show minimal FRβ expression in lung macrophages under basal conditions, but a substantial increase in FRβ expression after intratracheal LPS.

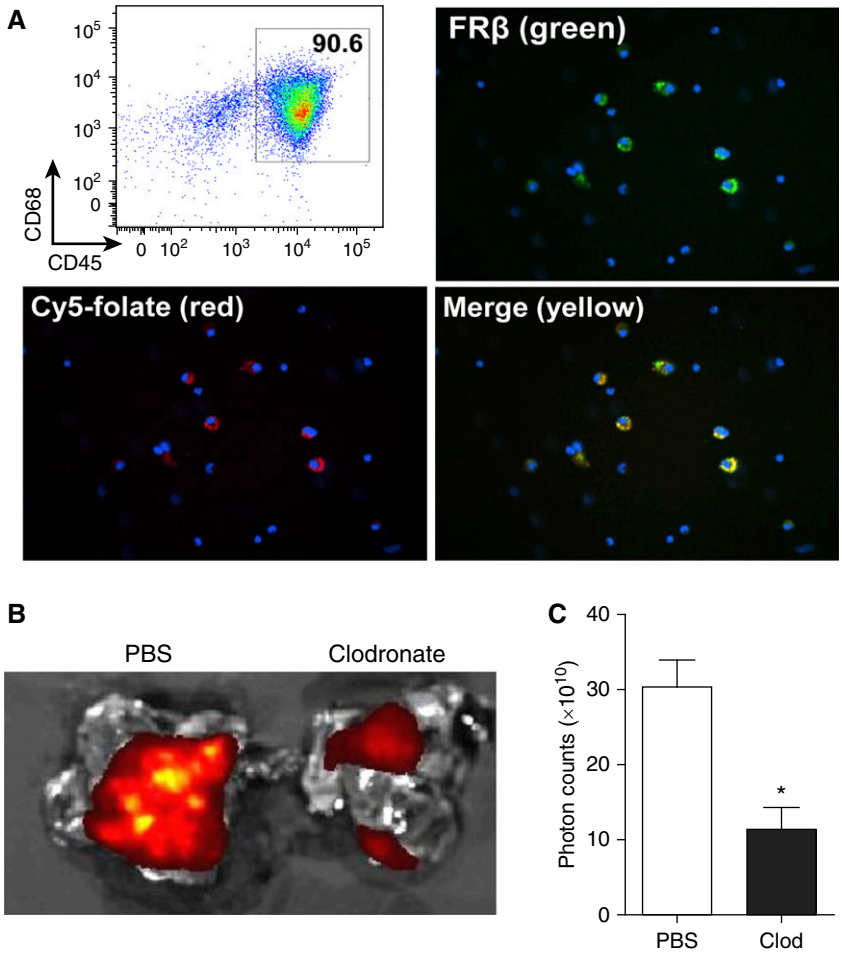


**Figure 3.** Activated lung macrophages are responsible for the uptake of folate-PEG-Cy5. At 48 hours after intratracheal LPS (3 μg/g body weight), total lung macrophages were isolated from lung lysates by adherence to tissue culture dishes for 2 hours and incubated with Cy5-PEG-folate (50 nM) for 30 minutes at 37°C. (*A*) Flow cytometry indicating that over 90% of adherent cells were macrophages (CD45$^+$/CD68$^+$). Representative microphotographs demonstrating colocalization of FRβ expression and folate uptake (*yellow*) in lung macrophages. (*B*) Representative *ex vivo* images showing folate-PEG-Cy-5–derived lung fluorescence and (*C*) photon counts from lungs of LPS-treated mice given control (PBS) or clodronate (Clod) liposomes (mean ± SEM; $n = 3$–6 per group; *$P < 0.05$).

### Imaging of Activated Macrophages Based on Folate Uptake

Because FRβ binds and facilitates folate endocytosis, we explored whether we could use uptake of a folic acid derivative (Cy5-PEG-folate) to image FRβ-expressing macrophages. Based on initial studies regarding clearance of Cy5-PEG-folate from the lung, we conducted *in vivo* imaging of mice at 1 hour after intratracheal delivery of Cy5-PEG-folate (500 nmol/kg) to measure folate uptake after LPS treatment. As shown in Figures 2A and 2B, LPS-treated mice exhibited increased lung fluorescence that peaked at 48 hours after intratracheal LPS, and returned to near baseline by 120 hours, similar to the time course for macrophage influx in this model. Because the chest wall causes substantial attenuation of the signal during the optical imaging (24), we

performed additional studies for *ex vivo* imaging determination of Cy5-PEG-folate–derived fluorescence. Consistent with results from *in vivo* imaging, these studies showed peak fluorescent intensity of the lungs at 48 hours after LPS injection (Figures 2C and 2D). To confirm that the fluorescent signal originated from macrophage uptake of labeled folate, we prepared frozen sections from lungs after *ex vivo* imaging and analyzed lung sections costained with 4′,6-diamidino-2-phenylindole using dual fluorescence confocal microscopy. As shown in Figure 2E, Cy5 fluorescence appeared exclusively in lungs of LPS-treated mice and localized to parenchymal cells with the appearance of macrophages.

To test how the route of injection of Cy5-PEG-folate affects imaging in the lungs, we also performed imaging studies in LPS-treated mice after delivery of the fluorescent probe by intravenous injection. Compared with studies with intratracheal delivery of the conjugated folate probe, intravenous probe delivery resulted in a similar time course with peak chest fluorescence at 48 hours after intratracheal LPS; however, the increase in chest fluorescence compared with baseline (no LPS) was lower with intravenous probe delivery (*see* Figures E1A–E1C in the online supplement). To confirm that the fluorescent signal was specific for folate uptake, we obtained a control probe (Cy5-PEG-N-hydroxysuccinimide, 500 nmol/kg) and performed imaging in control and intratracheal LPS–treated mice. With the control probe, the fluorescent signal over the chest was not different between control and LPS-treated mice, confirming the specificity of our conjugated folate probe (Figures E2A and E2B).

### Activated Interstitial Macrophages and Monocytes Uptake Labeled Folate via FRβ

To determine whether FRβ expression by activated macrophages was responsible for increased folate uptake after LPS, macrophages from whole lung tissue of intratracheal LPS–treated mice (48 h) were purified and incubated with Cy5-PEG-folate (50 nM) for 30 minutes at 37°C. We then performed colocalization of Cy5-PEG-folate uptake and FRβ fluorescence immunostaining. As shown in Figure 3A (*upper left*), over 90% of adherent cells expressed CD45 and CD68, identifying them as macrophages. By dual immunofluorescence, we found substantial colocalization of Cy5-PEG-folate uptake and FRβ expression in macrophages from LPS-treated mice (Figure 3A). In contrast, folate uptake and FRβ expression in control macrophages were minimal (data not shown). To confirm that pulmonary macrophages account for *in vivo* Cy5-PEG-folate–derived fluorescence, we imaged

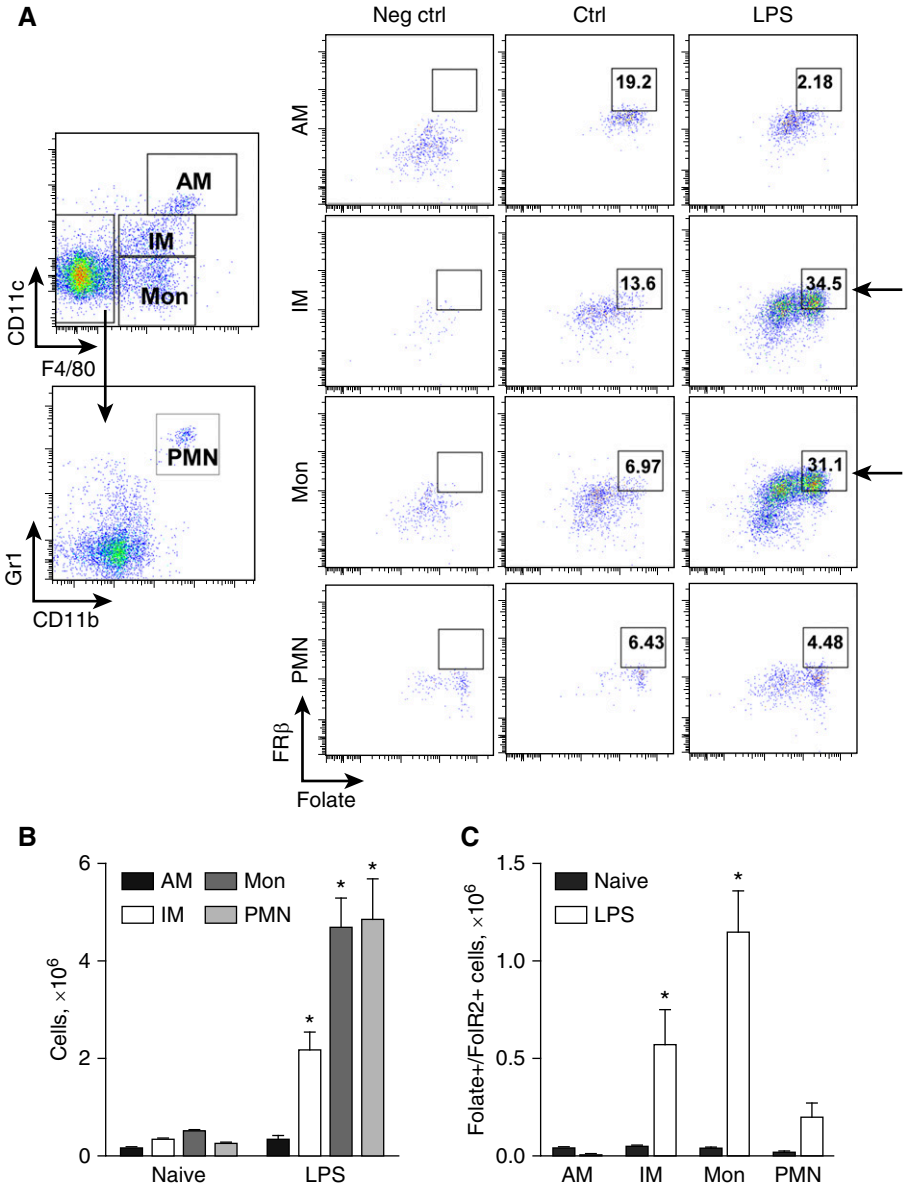


**Figure 4.** Pulmonary interstitial macrophages and monocytes are responsible for the increased uptake of folate-PEG-Cy5 via FRβ during LPS-induced airway inflammation. (*A*) Flow cytometry demonstrates FRβ-dependent folate-PEG-Cy5 uptake by viable/CD45$^+$/CD11c$^{hi}$/F4/80$^+$ alveolar macrophages (AMs), viable/CD45$^+$/CD11c$^{low}$/F4/80$^+$ interstitial macrophages (IMs), viable/CD45$^+$/CD11c$^-$/F4/80$^+$ monocytes (Mons), and viable/CD45$^+$/CD11b$^+$/Gr1$^{hi}$/F4/80$^-$ PMNs collected from mouse lungs at 48 hours after intratracheal LPS (3 μg/g body weight). Control mice (Ctrl) were treated with PBS by intratracheal injection. Negative control (Neg ctrl)—flow cytometry control sample stained with viability dye, CD45, CD11b, CD11c, Gr1, and F4/80 antibodies (no FRβ antibodies and folate-PEG-Cy5 added). (*B*) The number of viable/CD45$^+$/CD11c$^{hi}$/F4/80$^+$ AMs, viable/CD45$^+$/CD11c$^{low}$/F4/80$^+$ IMs, viable/CD45$^+$/ CD11c$^-$/F4/80$^+$ Mons, and viable/CD45$^+$/CD11b$^+$/Gr1$^{hi}$/F4/80$^-$ PMNs per mouse lung, and (*C*) the number of AMs, IMs, Mons, and PMNs exhibiting FRβ-dependent uptake of folate-PEG-Cy5 at 48 hours after intratracheal injection of LPS (3 μg/g body weight; each point represents the mean ± SEM; $n = 4$ per group; *$P < 0.001$).

mice after depletion of macrophages by liposomal clodronate. Previous studies have shown that combined intravenous and intratracheal delivery of liposomal clodronate results in approximately 90% depletion of lung macrophages (1, 22). For these studies, intratracheal LPS- and clodronate (or PBS)-containing liposomes were injected into mice 48 hours before imaging. Mice treated with clodronate showed a marked attenuation of lung fluorescence (Figures 3B and 3C), indicating that pulmonary macrophages account for the majority of folate uptake in the lungs after LPS treatment.

To determine which subpopulations of lung myeloid cells were responsible for LPS-induced folate uptake, we performed flow cytometry of cells isolated from control mice and mice treated with intratracheal LPS (48 h) after *ex vivo* incubation with Cy5-PEG-folate (50 nM). Using our recently published strategy for characterization of murine lung myeloid cell subsets (25), we found that F4/80$^{+}$/CD11c$^{low}$ interstitial macrophages and F4/80$^{+}$/CD11c$^{neg}$ monocytes were significantly increased in LPS-treated mice, and represented the major cell populations responsible for FRβ expression and folate uptake (Figures 4A and 4C). In contrast, no increase in the number of FRβ-expressing alveolar macrophages or neutrophils was identified after intratracheal LPS (Figure 4A). Together, our studies indicate that interstitial macrophages and monocytes are the major myeloid cell subsets that express FRβ and efficiently take up folate in the lungs after LPS treatment.

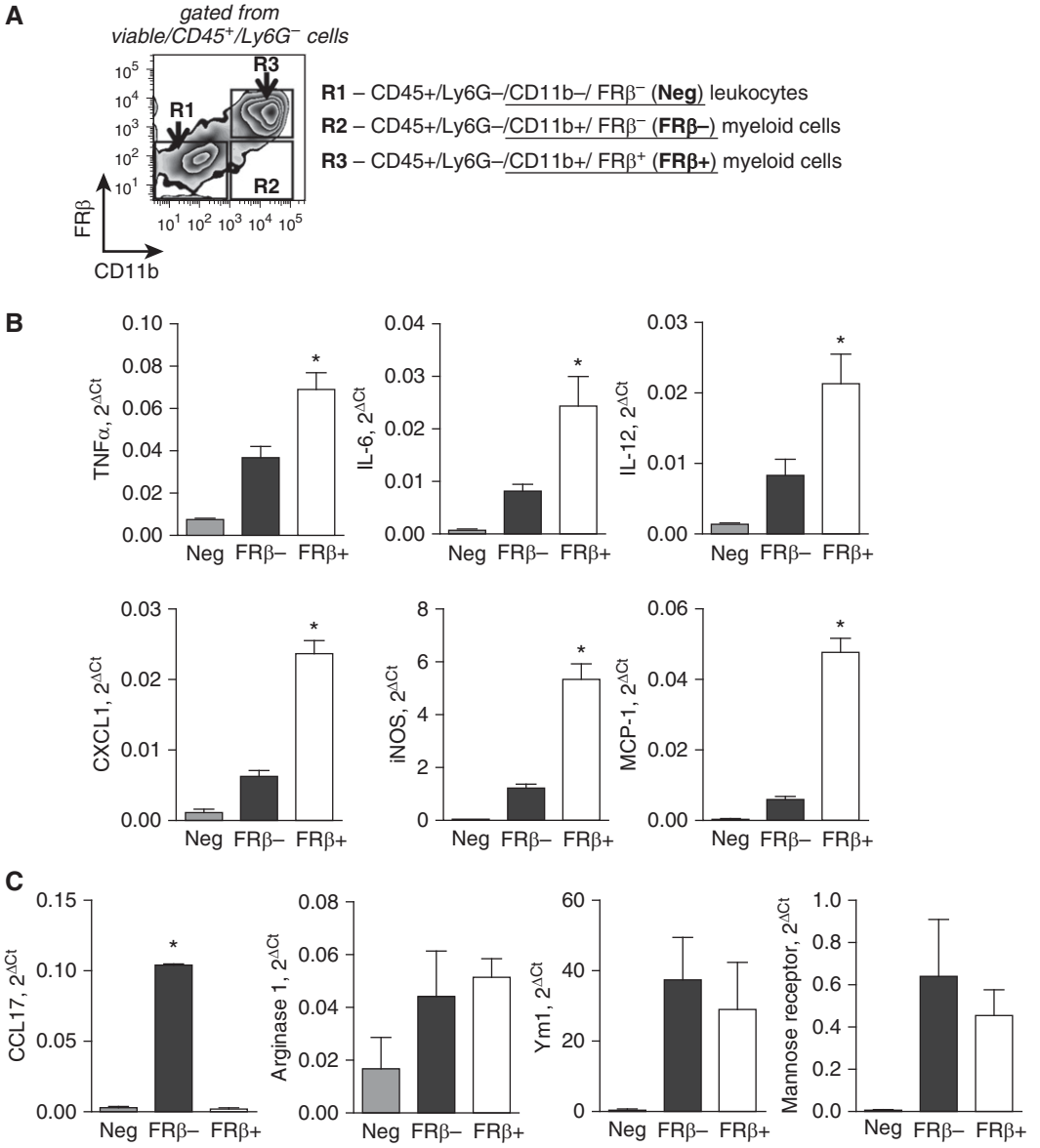


**Figure 5.** FRβ$^{+}$ macrophages/monocytes possess an M1 proinflammatory phenotype. (*A*) Strategy for sorting of viable CD45$^{+}$/Ly6G$^{-}$/CD11b$^{+}$/ FRβ$^{+}$ (FRβ+) macrophages, CD45$^{+}$/Ly6G$^{-}$/CD11b$^{+}$/FRβ$^{-}$ (FRβ$^{-}$) macrophages, and CD45$^{+}$/Ly6G$^{-}$/CD11b$^{-}$/FRβ$^{-}$ (Neg) leukocytes. (*B*) mRNA expression of TNF-α, IL-6, IL-12, chemokine (C-X-C motif) ligand 1 (CXCL1), inducible nitric oxide synthase (iNOS), and monocyte chemotactic protein (MCP-1). (*C*) mRNA expression of chemokine (C-C motif) ligand 17 (CCL17), arginase 1, Ym1, and mannose receptor by FRβ-positive or -negative macrophages, and FRβ-negative nonmyeloid lung leukocytes (mean ± SEM; $n = 4$ per group; $^{*}P < 0.001$).

### FRβ-Expressing Myeloid Cells Have a Proinflammatory Phenotype

To identify functional characteristics of FRβ$^+$ macrophages present in the lungs at 48 hours after intratracheal LPS, we selected CD45$^+$ leukocytes by FACS and then sorted Ly6G$^-$/CD11b$^-$ cells (which included alveolar macrophages and nonmyeloid leukocytes) and Ly6G$^-$/CD11b$^+$ cells (including interstitial macrophages and monocytes). CD45$^+$/Ly6G$^-$/CD11b$^+$ cells were further divided into two groups based on FRβ expression (Figure 5A). Neutrophils were excluded from the analysis as Ly6G$^+$/CD11b$^+$ cells. As demonstrated in Figure 5B, mRNA expression of proinflammatory M1 markers, including TNF-α, IL-12, IL-6, CXCL1, inducible nitric oxide synthase (iNOS), and monocyte chemotactic protein (MCP-1), was significantly increased in FRβ$^+$ monocytes/macrophages compared with FRβ$^-$ monocytes/macrophages and Ly6G$^-$/CD11b$^-$ leukocytes. Although expression of CCL17 mRNA by CD45$^+$/CD11b$^+$/FRβ$^+$ monocytes/macrophages was significantly lower in comparison to CD45$^+$/CD11b$^+$/FRβ$^-$ cells, we found no difference in expression of other macrophage M2 markers between these cell populations (Figure 5C). These findings indicate that FRβ$^+$ monocytes/interstitial macrophages induced by intratracheal LPS have proinflammatory M1 characteristics.

### CCR2 Mediates Recruitment and/or Activation of FRβ-Expressing Myeloid Cells after Intratracheal LPS

MCP-1 and its receptor, CCR2, play pivotal roles in recruitment of monocytes/macrophages during infection and other inflammatory conditions (26). Because we found that FRβ$^+$ monocytes/interstitial macrophages in the lung were significantly increased after intratracheal LPS, and that these cells expressed MCP-1, we wondered whether increased folate uptake in the lungs after intratracheal LPS depends on cell recruitment and/or activation via the MCP-1/CCR2 axis. To address this issue, wild-type (WT) and CCR2 KO mice were imaged after delivery of Cy5-PEG-folate by intratracheal injection in control mice and mice at 48 hours after intratracheal LPS. Although control CCR2 KO mice had similar lung fluorescence compared with WT mice after delivery of Cy5-PEG-folate, the LPS-induced increase in fluorescence over the lungs was markedly attenuated in CCR2 KO mice (Figures 6A and 6B). Lower fluorescence in lungs from CCR2 KO mice was confirmed by imaging of lungs *ex vivo* (Figures 6C and 6D). Consistent with these results, macrophages isolated from LPS-treated CCR2 KO mice expressed significantly less FRβ in comparison to macrophages from LPS-injected WT mice (Figure 6E).

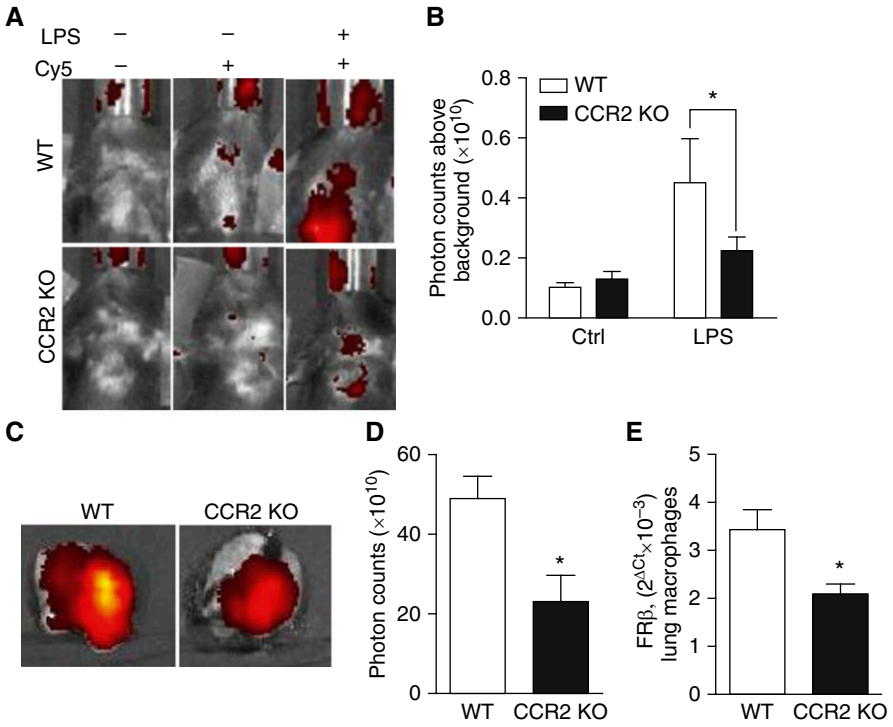


**Figure 6.** CC chemokine receptor (CCR) 2 deficiency attenuates lung macrophage FRβ expression and uptake of folate-PEG-Cy5 in mice treated with LPS. (*A*) Representative images showing folate-PEG-Cy5–derived chest fluorescence and (*B*) quantification of folate-PEG-Cy5–derived photon counts over the chest in wild-type (WT) and CCR2 knockout (KO) mice at 48 hours after intratracheal injection of LPS (3 μg/g body weight). Imaging was done at 1 hour after intratracheal injection of folate-PEG-Cy5 (500 nmol/kg). Results were normalized to background fluorescence in mice before injection of folate-PEG-Cy5. (*C*) Representative images of folate-PEG-Cy5–derived *ex vivo* lung fluorescence and (*D*) quantification of folate-PEG-Cy5–derived photon emission from lungs of WT and CCR2 KO mice at 48 hours after intratracheal injection of LPS (3 μg/g body weight). (*E*) mRNA expression of FRβ in total lung macrophages from WT and CCR2 KO mice at 48 hours after intratracheal LPS (mean ± SEM; $n = 4$–6 per group; $^*P < 0.01$).

### NF-κB–Dependent Inflammation Results in Increased FRβ Expression and Folate Uptake in Lung Macrophages

To determine whether FRβ expression marks activated macrophages in models other than LPS-induced airway inflammation, we performed imaging studies using a transgenic mouse model (IKTA) developed in our laboratory in which an activator of NF-κB is inducibly expressed in airway epithelium by the addition of dox to drinking water (19). In this model, 3 days of continuous transgene expression results in airway inflammation with increased numbers of neutrophils and macrophages. To test whether FR-based molecular imaging identifies activated macrophages in this model, we treated WT and IKTA mice with dox and imaged mice for folate uptake 3 days later (*in vivo* imaging 1 h after intratracheal injection of Cy5-PEG-folate). As shown in Figures 7A and 7B, the fluorescence signal over the chest was significantly increased in dox-treated IKTA compared with dox-treated WT mice. *Ex vivo* imaging confirmed the increased signal in lungs of dox-treated IKTA mice (Figures 7C and 7D). Macrophages isolated from IKTA mice at Day 3 after initiation of dox treatment demonstrated markedly increased FRβ expression (Figure 7E). In addition, we assessed monocyte/macrophage

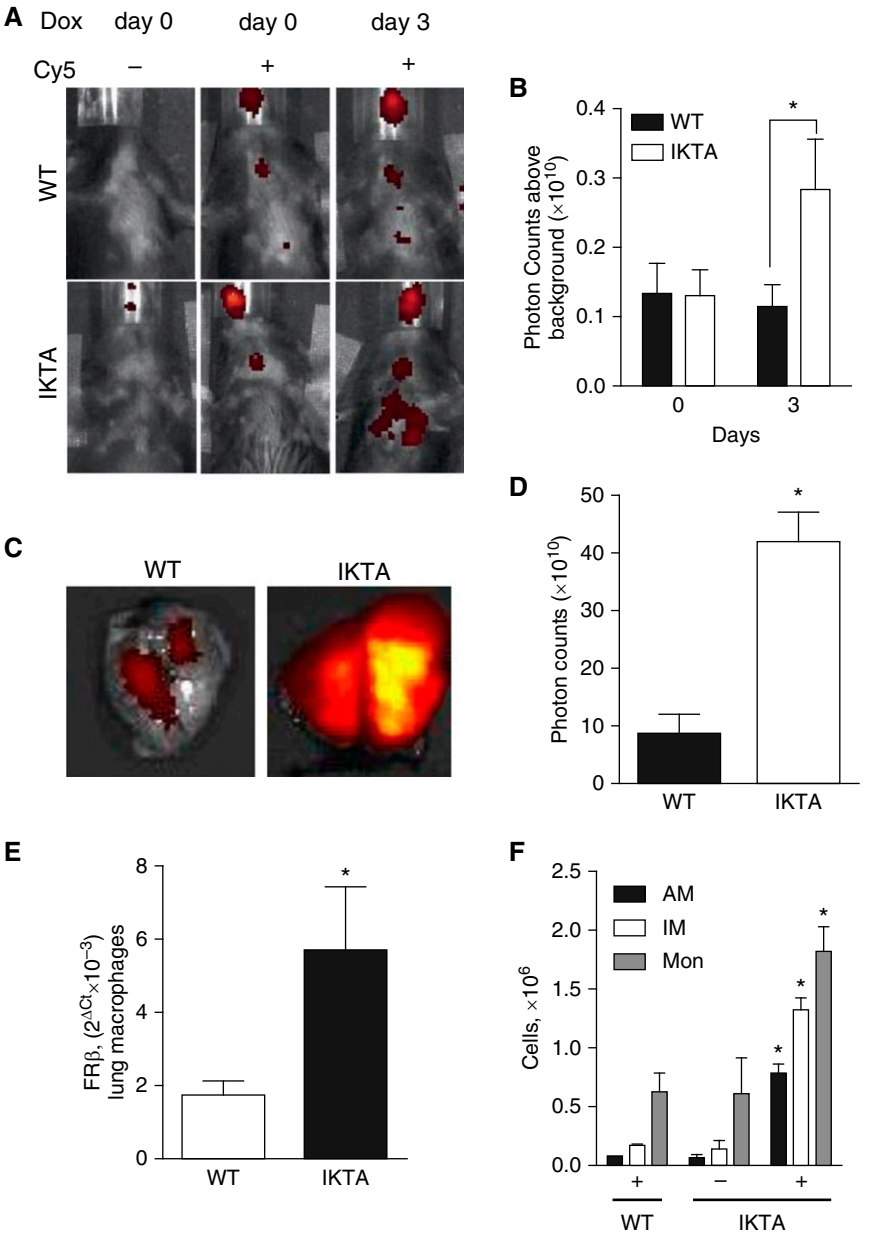


**Figure 7.** NF-κB activation in airway epithelium increases FRβ expression and resulting folate-PEG-Cy5 uptake in mice. (*A*) Representative images showing folate-PEG-Cy5–derived chest fluorescence. (*B*) Quantification of folate-PEG-Cy5–derived photons over the chest in WT and IKKβ *trans*-activated (IKTA) mice at baseline and on Day 3 after induction of NF-κB activity in airway epithelium by treatment with doxycycline (dox). Images were taken at 1 hour after intratracheal injection of folate-PEG-Cy5 (500 nmol/kg), and photon counts were normalized to background fluorescence (mice were imaged before the injection of intratracheal folate-PEG-Cy5). (*C*) Representative images showing folate-PEG-Cy5–derived *ex vivo* lung fluorescence. (*D*) Quantification of folate-PEG-Cy5–derived photons emitted from lungs of WT and IKTA mice 3 days after initiation of dox treatment. (*E*) mRNA expression of FRβ in total lung macrophages isolated from WT and IKTA mice after 3 days of NF-κB activation with dox. (*F*) The number of macrophages/monocytes identified by flow cytometry in lungs from WT and IKTA mice 3 days after initiation of treatment with dox (mean ± SEM; $n = 5$ per group; $^*P < 0.05$).

subsets in lungs by flow cytometry and found a significant increase in alveolar macrophages, interstitial macrophages, and monocytes in IKTA mice after activation of NF-κB signaling in airway epithelium (Figure 7F). To determine which myeloid cell subsets were responsible for FRβ expression and folate uptake in IKTA mice, we performed flow cytometry studies using cells isolated from lungs of dox-treated WT and IKTA mice. As shown in Figures E3A and E3B, interstitial macrophages and monocytes from IKTA mice had significantly increased folate uptake and FRβ expression after 3 days of dox treatment. Together, these studies show similar findings to the intratracheal LPS model, and suggest that FRβ expression may be induced in myeloid cell populations in the lungs after different inflammatory stimuli.

## Discussion

These studies establish detection of folate uptake via FRβ expression as a viable methodology for molecular imaging of activated macrophages in the lungs during acute lung inflammation. During basal conditions, minimal FRβ expression in lung macrophages correlates with low levels of folate uptake in the lungs. However, after induction of inflammation by LPS or activation of NF-κB in airway epithelium, folate uptake is substantially increased by FRβ-expressing interstitial macrophages and pulmonary monocytes. Increased folate uptake translates directly into increased retention of a folate-linked fluorescent probe delivered by the intratracheal or intravenous route, which can be identified by *in vivo* fluorescence imaging. The fluorescent signal is cell type–specific, as mature alveolar macrophages and neutrophils do not contribute significantly to increased uptake of folate in this setting. FRβ$^+$ expression is associated with expression of a proinflammatory mediator profile characteristic of classically activated macrophages, thus identifying cells that contribute to the acute inflammatory response in the lungs. During acute inflammation, circulating monocytes leave the bloodstream and migrate into tissues where, after conditioning by local mediators, they differentiate into macrophages. Migration of macrophages/monocytes to areas of inflammation and injury is largely mediated through chemokines and their receptors, particularly CCR2 (27, 28). By studying CCR2 KO mice, we showed that recruitment and activation of FRβ$^+$ macrophages/monocytes in the lungs is dependent on the MCP-1/CCR2 axis. In combination, our findings support the conclusion that folate-based imaging is an

effective method for detecting activated M1-like macrophages/monocytes recruited to the lungs during acute lung inflammation. This methodology may facilitate noninvasive monitoring of macrophage activation during acute lung inflammation, thus enabling a better understanding of inflammatory processes at various stages of acute lung inflammation/injury.

Although the functional importance of FRβ expression is not entirely clear, inflammatory stimuli promote glycolysis in macrophages because of increased energy requirements (29). The glycolysis pathway requires folate for one-carbon metabolism (30); therefore, we speculate that activated macrophages express FRβ due to increased folate demand for generation of ATP. Although FRβ-expressing macrophages have been identified in inflamed human joints and several animal models of inflammatory diseases (11, 15, 16), our study provides new information regarding functional subsets and phenotype of myeloid cells expressing the receptor and how these cells are recruited to the lungs. In addition, by depleting macrophages, we definitively show that myeloid lineage cells are indeed the target for uptake of folate probe via this receptor. In a prior study, it was suggested that FRβ$^+$ expression correlates with classical activation markers in peritoneal macrophages elicited by bacteria, thyoglycollate, or zymosan, including CD80, CD86, and TNF-α, and produce reactive oxygen species (8). Consistent with these observations, our data revealed that FRβ$^+$ macrophages from LPS-treated lungs produce mediators consistent with M1 polarized cells. In contrast, other studies have reported that FRβ$^+$ macrophages coexpress M2 markers in tumor-associated macrophages (9) and in a murine model of asthma (31). In humans, a recent publication found that proinflammatory monocytes (CD14$^{high}$, CD16$^-$) were the predominant cell population that expresses functional FRβ in peripheral blood (32). However, FRβ$^+$ macrophages have been shown to express a mixed pattern of M1 and M2 markers in synovial tissue from patients with osteoarthritis and rheumatoid arthritis (33). Based on available data, it appears that the precise phenotype of FRβ$^+$ myeloid cells may depend on the local microenvironment, as well as the activating stimulus. In addition, it appears that FRβ expression, like many other macrophage markers and mediators, may not always fit neatly into the prevailing categorization of M1 or M2 macrophage activation.

Molecular imaging techniques can be used to monitor the inflammatory response *in situ*. In particular, targeting selected markers to specific cells can provide accurate measurements of disease activity (34). In addition to FRβ, other options for molecular imaging of macrophages *in vivo* include use of ultrasmall paramagnetic iron oxide particles in magnetic resonance imaging, anti-CD14$^+$ antibody–labeled tracers, nanoparticles, and probes targeting the peripheral benzodiazepine receptor (35–37). Our approach for delivery of Cy5-conjugated folate is effective for detecting activated macrophages in the lungs of mice, but this specific approach is not applicable to larger animals, including humans, because of limited tissue penetration of *in vivo* fluorescent imaging. Therefore, use of folate-based methodologies in humans requires development and testing of imaging probes, such as radiolabeled positron emission tomography probes, that overcome this limitation. To date, most studies in humans related to folate imaging have focused on radiodiagnostic imaging approaches for detection of tumors, which can express FRα on the surface of cancer cells (15). An imaging test, called FolateScan, using a technetium-99–labeled folate derivative ($^{99m}$Tc-EC20), has been developed for use in patients with FR-positive cancer (8, 38). In addition, PET probes using $^{18}$F-folate derivatives have been developed for imaging FR-positive tumors (39). This imaging approach has also been used to identify inflamed joints in patients with rheumatoid arthritis (40). Together with our current study, available information suggests the feasibility of developing folate-based molecular imaging strategies based on these technologies that could be applied for monitoring and investigating pathologies of inflammatory lung diseases in humans.

In conclusion, these studies identify a new approach for quantifying and sequentially monitoring lung inflammation based on activation of FRβ expression and increased folate uptake in classically activated pulmonary monocytes/macrophages. This promising methodology for molecular imaging of inflammation may be applicable to other inflammatory lung diseases in animals and humans. ■

**Author disclosures** are available with the text of this article at www.atsjournals.org.

## References


1. Koay MA, Gao X, Washington MK, Parman KS, Sadikot RT, Blackwell TS, Christman JW. Macrophages are necessary for maximal nuclear factor-kappaB activation in response to endotoxin. *Am J Respir Cell Mol Biol* 2002;26:572–578.
2. Blackwell TS, Lancaster LH, Blackwell TR, Venkatakrishnan A, Christman JW. Differential NF-kappaB activation after intratracheal endotoxin. *Am J Physiol* 1999;277:L823–L830.
3. Koay MA, Christman JW, Wudel LJ, Allos T, Cheng DS, Chapman WC, Blackwell TS. Modulation of endotoxin-induced NF-kappa B activation in lung and liver through TNF type 1 and IL-1 receptors. *Am J Physiol Lung Cell Mol Physiol* 2002;283:L1247–L1254.
4. Han W, Joo M, Everhart MB, Christman JW, Yull FE, Blackwell TS. Myeloid cells control termination of lung inflammation through the NF-kappaB pathway. *Am J Physiol Lung Cell Mol Physiol* 2009;296: L320–L327.
5. Parsons PE, Eisner MD, Thompson BT, Matthay MA, Ancukiewicz M, Bernard GR, Wheeler AP; NHLBI Acute Respiratory Distress Syndrome Clinical Trials Network. Lower tidal volume ventilation and plasma cytokine markers of inflammation in patients with acute lung injury. *Crit Care Med* 2005;33:1–6, discussion 230–232.
6. Meduri GU, Annane D, Chrousos GP, Marik PE, Sinclair SE. Activation and regulation of systemic inflammation in ARDS: rationale for prolonged glucocorticoid therapy. *Chest* 2009;136:1631–1643.
7. Meduri GU, Muthiah MP, Carratu P, Eltorky M, Chrousos GP. Nuclear factor-kappaB– and glucocorticoid receptor alpha–mediated mechanisms in the regulation of systemic and pulmonary inflammation during sepsis and acute respiratory distress syndrome: evidence for inflammation-induced target tissue resistance to glucocorticoids. *Neuroimmunomodulation* 2005;12:321–338.
8. Xia W, Hilgenbrink AR, Matteson EL, Lockwood MB, Cheng JX, Low PS. A functional folate receptor is induced during macrophage activation and can be used to target drugs to activated macrophages. *Blood* 2009;113:438–446.
9. Puig-Kröger A, Sierra-Filardi E, Domínguez-Soto A, Samaniego R, Corcuera MT, Gómez-Aguado F, Ratnam M, Sánchez-Mateos P, Corbí AL. Folate receptor beta is expressed by tumor-associated macrophages and constitutes a marker for M2 anti-inflammatory/regulatory macrophages. *Cancer Res* 2009;69:9395–9403.

10. Nagai T, Tanaka M, Hasui K, Shirahama H, Kitajima S, Yonezawa S, Xu B, Matsuyama T. Effect of an immunotoxin to folate receptor beta on bleomycin-induced experimental pulmonary fibrosis. *Clin Exp Immunol* 2010;161:348–356.
11. Piscaer TM, Müller C, Mindt TL, Lubberts E, Verhaar JA, Krenning EP, Schibli R, De Jong M, Weinans H. Imaging of activated macrophages in experimental osteoarthritis using folate-targeted animal single-photon-emission computed tomography/computed tomography. *Arthritis Rheum* 2011;63:1898–1907.
12. Varghese B, Haase N, Low PS. Depletion of folate-receptor–positive macrophages leads to alleviation of symptoms and prolonged survival in two murine models of systemic lupus erythematosus. *Mol Pharm* 2007;4:679–685.
13. Clifford AJ, Arjomand A, Dueker SR, Schneider PD, Buchholz BA, Vogel JS. The dynamics of folic acid metabolism in an adult given a small tracer dose of 14C-folic acid. *Adv Exp Med Biol* 1998;445:239–251.
14. Zhao R, Diop-Bove N, Visentin M, Goldman ID. Mechanisms of membrane transport of folates into cells and across epithelia. *Annu Rev Nutr* 2011;31:177–201.
15. Leamon CP, Jackman AL. Exploitation of the folate receptor in the management of cancer and inflammatory disease. *Vitam Horm* 2008; 79:203–233.
16. Feng Y, Shen J, Streaker ED, Lockwood M, Zhu Z, Low PS, Dimitrov DS. A folate receptor beta–specific human monoclonal antibody recognizes activated macrophage of rheumatoid patients and mediates antibody-dependent cell–mediated cytotoxicity. *Arthritis Res Ther* 2011;13:R59.
17. Paulos CM, Turk MJ, Breur GJ, Low PS. Folate receptor–mediated targeting of therapeutic and imaging agents to activated macrophages in rheumatoid arthritis. *Adv Drug Deliv Rev* 2004;56: 1205–1217.
18. Müller C, Forrer F, Schibli R, Krenning EP, de Jong M. SPECT study of folate receptor–positive malignant and normal tissues in mice using a novel $^{99m}$Tc-radiofolate. *J Nucl Med* 2008;49:310–317.
19. Cheng DS, Han W, Chen SM, Sherrill TP, Chont M, Park GY, Sheller JR, Polosukhin VV, Christman JW, Yull FE, *et al*. Airway epithelium controls lung inflammation and injury through the NF-kappa B pathway. *J Immunol* 2007;178:6504–6513.
20. Lawson WE, Cheng DS, Degryse AL, Tanjore H, Polosukhin VV, Xu XC, Newcomb DC, Jones BR, Roldan J, Lane KB, *et al*. Endoplasmic reticulum stress enhances fibrotic remodeling in the lungs. *Proc Natl Acad Sci USA* 2011;108:10562–10567.
21. Degryse AL, Tanjore H, Xu XC, Polosukhin VV, Jones BR, McMahon FB, Gleaves LA, Blackwell TS, Lawson WE. Repetitive intratracheal bleomycin models several features of idiopathic pulmonary fibrosis. *Am J Physiol Lung Cell Mol Physiol* 2010;299:L442–L452.
22. Everhart MB, Han W, Parman KS, Polosukhin VV, Zeng H, Sadikot RT, Li B, Yull FE, Christman JW, Blackwell TS. Intratracheal administration of liposomal clodronate accelerates alveolar macrophage reconstitution following fetal liver transplantation. *J Leukoc Biol* 2005;77:173–180.
23. Maus UA, Wellmann S, Hampl C, Kuziel WA, Srivastava M, Mack M, Everhart MB, Blackwell TS, Christman JW, Schlöndorff D, *et al*. CCR2-positive monocytes recruited to inflamed lungs downregulate local CCL2 chemokine levels. *Am J Physiol Lung Cell Mol Physiol* 2005;288:L350–L358.
24. Schuster DP, Blackwell TS. Molecular imaging of the lung. Boca Raton, FL: Taylor & Francis Group Publishers; 2005.
25. Zaynagetdinov R, Sherrill TP, Kendall PL, Segal BH, Weller KP, Tighe RM, Blackwell TS. Identification of myeloid cell subsets in murine lungs using flow cytometry. *Am J Respir Cell Mol Biol* 2013;49: 180–189.
26. Yadav A, Saini V, Arora S. MCP-1: chemoattractant with a role beyond immunity: a review. *Clin Chim Acta* 2010;411:1570–1579.
27. Charo IF, Ransohoff RM. The many roles of chemokines and chemokine receptors in inflammation. *N Engl J Med* 2006;354: 610–621.
28. Tacke F, Randolph GJ. Migratory fate and differentiation of blood monocyte subsets. *Immunobiology* 2006;211:609–618.
29. O'Neill LAJ. A critical role for citrate metabolism in LPS signalling. *Biochem J* 2011;438:e5–e6.
30. Tedeschi PM, Markert EK, Gounder M, Lin H, Dvorzhinski D, Dolfi SC, Chan LL, Qiu J, DiPaola RS, Hirshfield KM, *et al*. Contribution of serine, folate and glycine metabolism to the ATP, NADPH and purine requirements of cancer cells. *Cell Death Dis* 2013;4:e877.
31. Shen J, Chelvam V, Cresswell G, Low PS. Use of folate-conjugated imaging agents to target alternatively activated macrophages in a murine model of asthma. *Mol Pharm* 2013;10:1918–1927.
32. Shen J, Hilgenbrink AR, Xia W, Feng Y, Dimitrov DS, Lockwood MB, Amato RJ, Low PS. Folate receptor-β constitutes a marker for human proinflammatory monocytes. *J Leukoc Biol* 2014;96: 563–570.
33. Tsuneyoshi Y, Tanaka M, Nagai T, Sunahara N, Matsuda T, Sonoda T, Ijiri K, Komiya S, Matsuyama T. Functional folate receptor beta–expressing macrophages in osteoarthritis synovium and their M1/M2 expression profiles. *Scand J Rheumatol* 2012;41:132–140.
34. Jones HA. Inflammation imaging. *Proc Am Thorac Soc* 2005;2: 545–548, 513–514.
35. Thorek DL, Chen AK, Czupryna J, Tsourkas A. Superparamagnetic iron oxide nanoparticle probes for molecular imaging. *Ann Biomed Eng* 2006;34:23–38.
36. Goupille P, Chevalier X, Valat JP, Garaud P, Perin F, Le Pape A. Macrophage targeting with $^{99m}$Tc-labelled J001 for scintigraphic assessment of experimental osteoarthritis in the rabbit. *Br J Rheumatol* 1997;36:758–762.
37. Hatori A, Yui J, Yamasaki T, Xie L, Kumata K, Fujinaga M, Yoshida Y, Ogawa M, Nengaki N, Kawamura K, *et al*. PET imaging of lung inflammation with [18F]FEDAC, a radioligand for translocator protein (18 kDa). *PLoS One* 2012;7:e45065.
38. Sega EI, Low PS. Tumor detection using folate receptor–targeted imaging agents. *Cancer Metastasis Rev* 2008;27:655–664.
39. Müller C, Schibli R. Folic acid conjugates for nuclear imaging of folate receptor–positive cancer. *J Nucl Med* 2011;52:1–4.
40. Al Jammaz I, Al-Otaibi B, Amer S, Okarvi SM. Rapid synthesis and *in vitro* and *in vivo* evaluation of folic acid derivatives labeled with fluorine-18 for PET imaging of folate receptor–positive tumors. *Nucl Med Biol* 2011;38:1019–1028.